Intrinsic Cytosolic Calcium Buffering Properties of Single Rat Cardiac Myocytes

Joshua R. Berlin,* José W. M. Bassani,‡ and Donald M. Bers‡

*Bockus Research Institute, Graduate Hospital, Philadelphia, Pennsylvania 19146, and ‡Department of Physiology, Loyola University School of Medicine, Maywood, Illinois 60153 USA

ABSTRACT Intracellular passive Ca^{2+} buffering was measured in voltage-clamped rat ventricular myocytes. Cells were loaded with indo-1 (K^+ salt) to an estimated cytosolic concentration of 44 ± 5 μM (Mean ± SEM, $n = 5$), and accessible cell volume was estimated to be 24.5 ± 3.6 pl. Ca^{2+} transport by the sarcoplasmic reticulum (SR) Ca-ATPase and sarcolemmal Na-Ca exchange was inhibited by treatment with thapsigargin and Na-free solutions, respectively. Extracellular [Ca^{2+}] was maintained at 10 mM and, in some experiments, the mitochondrial uncoupler "1799" was used to assess the degree of mitochondrial Ca^{2+} uptake. To perform single cell titrations, intracellular Ca^{2+} ($[Ca^{2+}]_i$) was increased progressively by a train of depolarizing voltage clamp pulses from −40 to +10 mV. The total Ca^{2+} gain with each pulse was calculated by integration of the Ca current and then analyzed as a function of the rapid change in $[Ca^{2+}]_i$ during the pulse. In the range of $[Ca^{2+}]_i$ from 0.1 to 2 μM, overall cell buffering was well described as a single lumped Michaelis-Menten type species with an apparent dissociation constant, K_D, of 0.63 ± 0.07 μM ($n = 5$) and a binding capacity, B_{max}, of 162 ± 15 μmol/l cell H_2O. Correction for buffering attributable to cytosolic indo-1 gives intrinsic cytosolic Ca^{2+} buffering parameters of $K_D = 0.96 \pm 0.18$ μM and $B_{max} = 123 \pm 18$ μmol/l cell H_2O. The fast Ca^{2+} buffering measured in this manner agrees reasonably with the characteristics of known rapid Ca buffers (e.g., troponin C, calmodulin, and SR Ca-ATPase), but is only about half of the total Ca^{2+} buffering measured at equilibrium. Inclusion of slow Ca buffers such as the Ca/Mg sites on troponin C and myosin can account for the differences between fast Ca^{2+} buffering in phase with the Ca current measured in the present experiments and equilibrium Ca^{2+} buffering. The present data indicate that a rapid rise of $[Ca^{2+}]_i$ from 0.1 to 1 μM during a contraction requires approximately 50 μM Ca^{2+} to be added to the cytosol.

INTRODUCTION

Changes in intracellular free [Ca^{2+}] ($[Ca^{2+}]_i$) mediate a broad spectrum of cellular activities in cardiac myocytes so that $[Ca^{2+}]_i$ is closely regulated by several mechanisms (Bers, 1991). To understand fully the mechanisms that regulate $[Ca^{2+}]_i$, it is not sufficient to simply study changes in $[Ca^{2+}]_i$ because almost all Ca^{2+} is bound at intracellular buffering sites. Thus, to study these Ca^{2+} regulatory mechanisms, it is necessary to understand changes in both free and bound Ca^{2+} in the cell (Bers and Berlin, 1994).

Ca^{2+} has the potential to bind at many sites within cardiac myocytes including proteins such as troponin, myosin, calmodulin, transport proteins (most notably the Ca-ATPase, and Na-Ca exchange mechanism), small molecules such as ATP and phosphocreatine and binding sites associated with the cell membrane (Fabiato, 1983). The Ca^{2+} binding characteristics of many of these cellular binding sites have been examined under in vitro conditions, and it has become clear that cellular buffers can be divided into two practical categories, Ca-specific sites and Ca/Mg sites (Robertson et al., 1981). Ca-specific sites appear to be largely unoccupied by divalent ions at resting $[Ca^{2+}]_i$ and $[Mg^{2+}]_i$, but become increasingly Ca^{2+}-bound as $[Ca^{2+}]_i$ rises. Because Ca^{2+} diffusion in this situation is likely to be rate-limiting for Ca^{2+} binding, these sites such as the Ca-specific sites of troponin and calmodulin may be considered "fast Ca buffers." Conversely, Ca/Mg sites appear to be largely occupied by divalent ion, either Ca^{2+} or Mg^{2+}, at resting $[Ca^{2+}]_i$ and $[Mg^{2+}]_i$. Increased Ca^{2+} binding to these sites occurs only after the dissociation of Mg^{2+}. Thus, these sites, such as the Ca/Mg sites of troponin and myosin, can be considered "slow Ca buffers." In general, fast Ca buffers are believed to bind significant amounts of Ca^{2+} in phase with the cardiac muscle $[Ca^{2+}]_i$ transient, whereas Ca^{2+} binding to slow buffers may lag significantly behind the waveform for changes in $[Ca^{2+}]_i$ (Robertson et al., 1981; Konishi and Berlin, 1993).

There are two potential difficulties in relating the in vitro binding characteristics to Ca^{2+} binding within the intact cell. First, Ca^{2+} binding affinity is likely to be affected by conditions in the cell, such as solution ionic strength (Ogawa, 1985), that are difficult to evaluate. Even more important, however, is the finding that the Ca^{2+} binding affinity of some of these proteins may be dependent on protein/protein interactions within the cell (Zot and Potter, 1987). To overcome the limitations of in vitro studies, Ca^{2+} binding has been performed in triton-skinned ventricular trabeculae to determine the myofilament Ca^{2+} and Mg^{2+} binding site affinities of troponin and myosin (Solaro et al., 1974; Pan and Solaro, 1987). However, these studies necessarily precluded the examination of total cytosolic Ca^{2+} buffering. More recently, Hove-Madsen and Bers (1993) examined Ca^{2+} binding in digitonin-permeabilized myocytes, which allowed total cytosolic buffering to be examined. Theses studies found that Ca^{2+} buffering could be described by a two-site Michaelis Menten equation that predicted a twofold higher buffering capacity than that predicted by compiling data from

Received for publication 18 April 1994 and in final form 23 June 1994.

Address reprint requests to Joshua R. Berlin, Ph.D., Bockus Research Institute, Graduate Hospital, 415 S. 19th St., Philadelphia, PA 19146.

0006-3495/94/10/1775/13 $2.00

in vitro studies (Fabiato, 1983), but considerably lower than the cytosolic Ca^{2+} buffering estimated by Pierce et al. (1985) in whole ventricular homogenate or by Wendt-Gallitelli and Isenberg (1990) using x-ray microprobe analysis.

The present study seeks to expand on these previous studies by examining Ca^{2+} buffering in single, intact myocytes with the goal of describing the fast Ca^{2+} buffering properties of the cytosol. This data would be useful in quantitatively describing Ca^{2+} fluxes in the cytosol during a $[Ca^{2+}]_i$ transient and, therefore, would be important for understanding Ca^{2+} regulatory processes in the myocyte.

Preliminary communication of this work has been published (Berlin et al., 1994).

MATERIALS AND METHODS

General

The experimental techniques used in this study are modifications of previously published methods (Bers et al., 1990; Konishi and Berlin, 1993). Male rats weighing 200–250 g were anesthetized with pentobarbital (100 mg/kg, i.p.), and single cardiac ventricular myocytes were enzymatically isolated by a modification of the method of Mitra and Morad (1985). After enzymatic digestion and dispersion, cells were stored in a 0.2 mM $CaCl_2$-containing Tyrode's solution at room temperature or at 6°C until used.

Cells were placed in an experimental chamber (Cannell and Lederer, 1986) on the stage of an inverted microscope (Diaphot, Nikon Inc., Garden City, NJ) and superfused with a normal Tyrode's solution (145Na,2Ca). Cells were voltage-clamped via a single electrode technique (Hamill et al., 1981) with patch pipettes of 1–2 MΩ resistance filled with a intracellular salt solution containing 60 μM indo-1(K salt). After formation of a gigOhm seal, zero current and background fluorescence were measured. The membrane patch under the pipette was then ruptured to establish a whole cell voltage clamp and allow indicator diffusion into the myocyte.

Equipment for fluorescence measurement

Light from a xenon arc (PTI Inc., South Brunswick, NJ) was collected and partially collimated before passing through a narrow-band interference filter centered at 360 nm (10 nm FWHM) and a neutral density filter (N.D. 0.6). The filtered light was then focused onto one end of a liquid light guide. The other end of the light guide was placed in the epifluorescence port of the microscope so that the image of the light guide formed by a lens was at the back image plane of a high N.A. oil immersion objective, which focused the ultraviolet light onto the cell. Incident light was limited to the area of the cell with an adjustable field stop. An electronic shutter (Vincent Electronics, Rochester, NY) also limited the exposure of the cell to ultraviolet light. Light from the Kohler illuminator of the microscope was used throughout the experiments to view the cell with a CCD camera (NEC Corp., Mountain View, CA) but was limited to wavelengths longer than 750 nm with a longpass interference filter.

Fluorescent light was filtered at 410 and 500 nm (40 nm FWHM) and measured simultaneously with photomultiplier tubes (Thorn EMI, Rockaway, NJ) after diverting light with wavelengths longer than 700 nm by dichroic mirrors. A field stop limited the view of the photomultiplier tubes to the area of the myocyte.

Membrane potential, current, and fluorescence were recorded on videotape (Instrutech VR-100, Elmont, NY). For analysis, fluorescence data were filtered at 30–100 Hz, and current at 1 KHz with an 8-pole Bessel filter before digitization (DT2801A, Data Translation, Inc., Marlboro, MA) using commercially available software (A2D+; Medical Systems, Greenvale, NY).

Calibration of Ca^{2+}-dependent changes in indo-1 fluorescence

In vitro calibrations of indo-1 were carried out on the experimental apparatus with a glass capillary approximately 100 μm in diameter (see Fig. 1 *A*). The calibration solution contained (in mM) 140 KCl, 1 $MgCl_2$, 5 EGTA (ethylene glycol-bis(β-aminoethyl ether)*N,N,N',N'*-tetraacetic acid), 0.020 indo-1 (K salt) and 10 mM PIPES (piperizine-*N,N'*-bis[2-ethanesulfonic acid]), pH 7.2. Various amounts of $CaCl_2$ were added to set free Ca^{2+} concentrations. Free ion concentrations were calculated with a computer program, MaxChelator, vers. 6.1 (written by Chris Patton, Hopkins Marine Station, Pacific Grove, CA), which used the equations from Fabiato and Fabiato (1979) and dissociation constants determined by Harrison and Bers (1987) and Martell and Smith (1974).

The optical and Ca^{2+} binding properties of Ca indicators are believed to be different in salt solutions and in the cellular environment because of indicator binding to cellular constituents (Konishi et al., 1988; Hove-Madsen and Bers, 1992). Because cytosolic indo-1 concentration was estimated (see below), it was particularly important to estimate how the optical properties of the indicator might change in the cell. Toward this end, two approaches were used to determine the Ca^{2+}-dependent optical properties of indo-1 in the cell. First, the calibration parameters, R_{min}, R_{max}, and β were determined in separate experiments according the method of Borzak et al. (1990). In brief, at the end of an experiment, myocytes loaded with indo-1 were superfused in a Ca^{2+}-free, EGTA (2.5 mM)-containing Tyrode's solution that included 25 μM of the ionophore, 4-Br A23187. After fluorescence intensities reached a steady-state level and R_{min} ($F410_{min}/F500_{min}$) was calculated, the superfusion solution was changed to a Ca-free, 1 mM $LaCl_3$-containing Tyrode's solution. In this solution, fluorescence reached a new steady-state ($F410_{max}$, $F500_{max}$). To convert these fluorescence intensities to R_{max} for Ca, the relative fluorescence intensities of indo-1 in the presence of saturating concentrations of Ca^{2+} and La^{3+} were determined separately and then conversion factors were calculated as $k410 = F410_{Ca}/F410_{La}$ and $k500 = F500_{Ca}/F500_{La}$. R_{max} was then calculated as $F410_{max} * k410/(F500_{max} * k500)$. The scaling factor, β, was calculated as $F500_{max} * k500/F500_{min}$. The dissociation constant was estimated from the in vitro calibrations described above.

To estimate the changes in indo-1 optical properties in the intracellular environment, in vitro calibrations were repeated with the addition of 20 mg/ml Aldolase, similar to Konishi et al. (1988). This protein concentration is high enough to bind almost all indo-1, in accordance with reports that fluorescent indicators are largely bound within the cell (Konishi et al., 1988; Blatter and Wier, 1990; Hove-Madsen and Bers, 1992). Control calibrations were carried out with protein-free solution containing 320 mM sucrose to correct for changes in solution viscosity (as determined with an Ostwald viscometer). In the absence of protein, indo-1 showed a significant Ca^{2+}-dependent change in fluorescence intensity at 410 nm; however, in the presence of Aldolase, fluorescence at this wavelength was unaffected by changes in $[Ca^{2+}]$. Fluorescence emission at 500 nm was also slightly decreased, and the apparent K_D for Ca^{2+} was shifted to twofold higher concentrations (the effect of changes in K_D on the calculation of cytosolic buffering is presented in Discussion). The apparent blue-shift in the isosbestic wavelength and decrease in Ca^{2+} affinity for indo-1 in the presence of Aldolase are similar to the effect of protein on fura-2 fluorescence (Konishi et al., 1988). In the cell, fluorescence at 410 nm was also close to the isosbestic wavelength. Thus, changes in indo-1 fluorescence in the presence of Aldolase are at least qualitatively similar to those observed in the cell.

Determination of accessible cytosolic volume

To calculate Ca^{2+} buffering in the cell, it was also necessary to determine the cytosolic volume that was accessible to Ca^{2+} ions. In spherical or cylindrical cells, the estimation of cell volume is quickly done by converting membrane capacitance to surface area. Unfortunately, cardiac myocytes do not have a simple geometry. T-tubules as well as membrane caveolae and plications are prominent features of rat ventricular myocytes (Sommer and Waugh, 1976; Page, 1978). Most cells in this study also displayed some degree of branching. Given these features (which increase cell surface area

but contribute little or nothing to cytosolic volume), it seemed unlikely that a simple conversion of cell capacitance to membrane surface area would yield an accurate estimate of cell volume.

To determine the relationship between cell capacitance (i.e., surface area) and cell volume, we attempted to calculate cell volume assuming that the idealized cell shape was a rectangular parallelepiped. Two of the three dimensions, cell length and width, could be accurately determined with an eyepiece reticle. Myocytes in this study were 116 ± 4 μm (Mean ± SEM, $n = 5$) in length and 23 ± 2 μm wide. Cell depth, on the other hand, was more difficult to estimate. Even so, maximum cell depth was estimated by determining the difference in the first and last in-focus image of the cell top and bottom surface, respectively, as viewed with a CCD camera (18 ± 2 μm). Given that cell depth is not accurately determined by this procedure, we attempted to arrive at a systematic manner to estimate average cell depth from accurately determined parameters, i.e., cell length, width, and capacitance.

Cell capacitance in this study averaged 168 ± 24 pF ($n = 5$), or an average surface area of 16,800 μm^2 (at 1 $\mu F/cm^2$). If it was assumed that 100% of cell capacitance represented surface membrane, average cell depth was calculated to be 42 ± 9 μm, clearly much larger than indicated by optical measurements. If t-tubular membrane was assumed to contribute 33% of total sarcolemma (Page, 1978), average cell depth was calculated to be 27 ± 7 μm. This depth, although smaller, was clearly at odds with the optical measurements that showed that cell depth was less than cell width. Thus, only accounting for t-tubular membrane would still lead to a significant overestimate of cell volume. As a final calculation, we assumed that sarcolemmal caveolae, etc. involved half as much membrane as the t-tubules so that a total of 50% of membrane was not surface membrane. Given these assumptions, average cell depth was calculated to be 14 ± 4 μm. This value, although slightly less than the optically observed maximum depth, is consistent with the observed cell dimensions. Preliminary experiments in rabbit and rat ventricular cells, not reported in this study, were also consistent with the dimensions reported here.

Total cell volume was thus estimated as length times width times average depth calculated under the assumption that 50% of cell capacitance represented surface membrane. Because mitochondria and other membrane bound organelles occupy a significant fraction of total cell volume (Page, 1978), accessible cell volume was estimated as 65% of total cell volume.

Determination of cell indo-1 concentration

In the present experiments, exogenous Ca^{2+} buffer, i.e., indo-1, was added to the cytosol. Thus, to estimate intrinsic cytosolic buffering, it is necessary to subtract Ca^{2+} buffering attributable to indo-1 from the total cytosolic Ca^{2+} buffering. The first step in determining indo-1 Ca^{2+} buffering was to determine the cytosolic concentration of the indicator. This was accomplished by estimating intracellular indo-1 concentration according to the procedure of Berlin and Konishi (1993), in which cell fluorescence is compared with fluorescence of a "standard cell." In the present experiments, the standard cell was a thin glass capillary (11 μm diameter, similar to calculated cell depth) containing 60 μM indo-1 in the same solution used in the voltage-clamping electrode ($[Ca^{2+}] \leq 100$ nM).

In brief, fluorescence intensity of the cell measured at 410 nm (the isosbestic wavelength) was divided by accessible volume (as determined above) to calculate cellular fluorescence per unit volume (CF). At the end of an experiment, the standard cell was placed in the same position as the cell and fluorescence intensity at 410 nm was measured and a standard fluorescence per unit volume (SF) was calculated. Cellular indo-1 concentration was then calculated as

$$[\text{indo}] = (\text{CF}/\text{SF}) * 60\ \mu\text{M} * 1/\phi, \quad (1)$$

where ϕ is the ratio of indo-1 fluorescence at 410 nm in the presence and absence of Aldolase at pCa = 7 (close to resting $[Ca^{2+}]$ levels) as determined in Fig. 1. The results of these calculations for each cell are listed in Table 1.

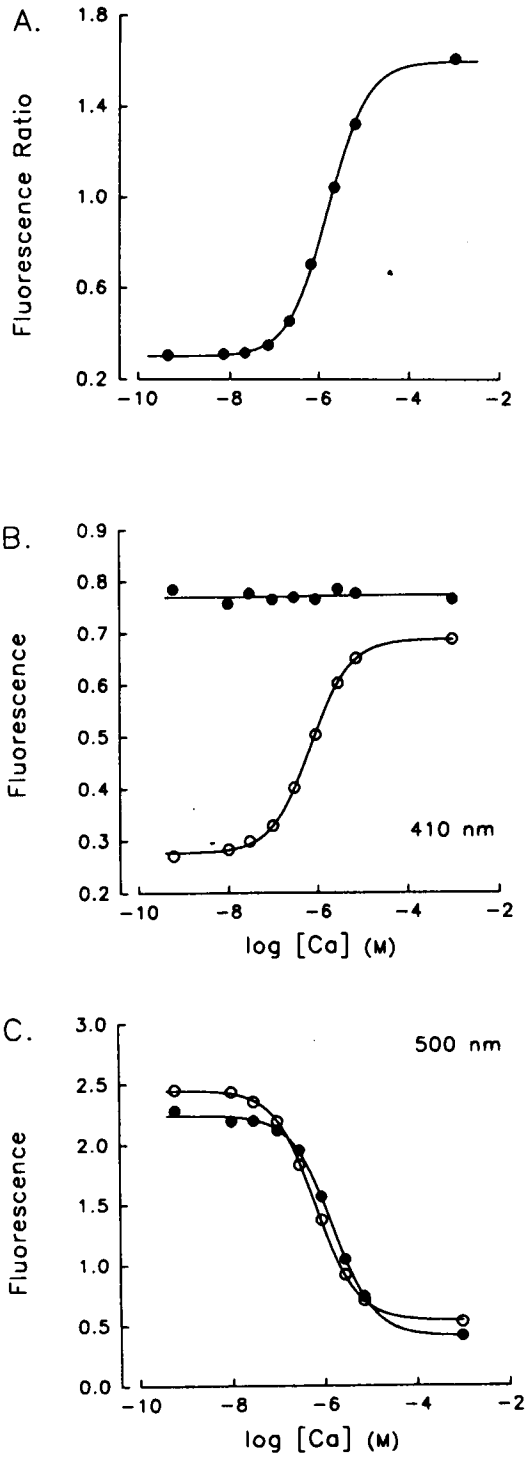

FIGURE 1 In vitro calibration of indo-1. (*A*) Dependence of fluorescence ratio on $[Ca^{2+}]$. Ca^{2+}-dependent changes in the ratio of fluorescence intensities (F410/F500) for indo-1 (20 μM) during illumination with 360 nm light were determined in a 100 μm diameter capillary on the same microscope used in the experiments. Free $[Ca^{2+}]$ in the EGTA-containing calibration solution was calculated as described in the text. The K_D(Ca) for indo-1 was 0.33 μM and β, was 4.8. (*B*) Effect of Aldolase on indo-1 fluorescence at 410 nm. The calibration in *A* was repeated except that 320 mM sucrose (○) or 20 mg/ml Aldolase (●) was included in the calibration solution. (*C*) Effect of Aldolase on indo-1 fluorescence at 500 nm. The same calibration as in *B* in the presence of sucrose (○) and Aldolase (●).

TABLE 1 Estimation of intrinsic Ca buffers in rat myocytes

		Total		Intrinsic§		
Cell #	Vol* (pl)	B_{max} (μmol/l)	K_D (μM)	[Indo-1]‡ (μmol/l)	B_{max} (μmol/l)	K_D (μM)
1	23.0	178¶	0.89¶	50	143¶	1.57¶
2	33.7	182	0.50	26	158	0.55
3	13.6	196	0.69	48	148	0.97
4	21.9	140‖	0.50‖	43‖	103‖	0.69‖
5	31.6	114	0.57	51	68	1.02
Mean	24.5	162	0.63	44	123	0.96
SEM	3.6	15	0.07	5	18	0.18

* Intracellular accessible volume was calculated as 65% of the total cell volume necessary to account for 50% of cell capacitance with known cell length and width.

‡ Cytosolic [indo-1] was estimated by measuring cell fluorescence, normalizing for intracellular accessible volume and comparing with the fluorescence of a standard indo-1 solution in a known volume.

§ Intrinsic cellular Ca buffers were estimated by assuming that total buffers were the sum of intrinsic buffers and indo-1, where indo-1 has a K_D = 0.33 μM.

¶ If the K_D(Ca) for indo-1 was assumed to be increased fourfold in the cell, total cytosolic Ca^{2+} buffers were calculated to have a B_{max} = 176 μmol/l and a K_D = 3.7 μM, and intrinsic buffers were calculated to have a B_{max} = 138 μmol/l and K_D = 6.3 μM, i.e., B_{max} remained unchanged, whereas buffer K_D increased fourfold.

‖ Estimation of cytosolic Ca^{2+} buffers was performed a second time in the presence of "1799." Total cytosolic Ca^{2+} buffers were calculated to have a B_{max} = 168 μmol/l and a K_D = 0.58 μM. Cytosolic [indo-1] had increased to 50 μmol/l so that intrinsic buffers were calculated to have a B_{max} = 119 μmol/l and a K_D = 0.76 μM.

Statistics

Nonlinear least-squares fitting was performed using a Marquardt-Levenberg algorithm routine included in SigmaPlot (Jandel Scientific, Corta Madera, CA). Equilibrium [Ca^{2+}] predicted from model buffers was calculated using a computer program, REACT, written by Godfrey L. Smith. Summary data are displayed as Mean ± SEM.

Solutions and materials

Myocytes were initially superfused with a Tyrode's solution (145Na,2Ca) containing (in mM) 140 NaCl, 4 KCl, 1 $MgCl_2$, 2 $CaCl_2$, 10 glucose and 10 HEPES (*N*-[2-hydroxyethyl]piperizine-*N'*-[2-ethanesulfonic acid]), pH 7.4. All experiments were performed at room temperature. To switch to an Na-free superfusion solution, Li was substituted for Na on an equimolar basis, pH was adjusted with LiOH and 1 mM EGTA was added to the solution. Na- and Ca-free solutions (0Na,0Ca) contained a total of 3–5 mM Mg to maintain clamp stability and prevent monovalent cation influx through Ca channels (Hess et al., 1986). Na-free, 10 mM Ca-containing solution (0Na, 10Ca) also contained 1 mM EGTA, but Mg was 1 mM, whereas total Ca was 11 mM. No adjustments for changes in ionic strength were made.

The intracellular salt solution in the voltage clamp electrode contained (in mM) 100 cesium glutamate, 20 CsCl, 1 $MgCl_2$, 5 MgATP, 5 phosphocreatine (ditris salt), 0.06 indo-1 (K salt), and 30 PIPES, pH 7.2.

All chemicals were reagent grade. Caffeine was purchased from Sigma Chemical Co. (St. Louis, MO) and dissolved directly in 145Na,2Ca solution at a final concentration of 20 mM. Thapsigargin (Calbiochem, San Diego, CA) was prepared as a 10 mM stock in dimethyl sulfoxide (DMSO) and dissolved in 145Na,2Ca solution at a final concentration of 2.5–10 μM just before use. The mitochondrial uncoupler "1799" (bis(hexafluoroacetonyl)-acetone) (generously provided by Dupont, Inc., Wilmington, DE and Dr. J. R. Williamson of the University of Pennsylvania) was dissolved in ethanol (10 mM) and diluted in 0Na,10Ca solution at a final concentration of 5 μM. Vehicles (DMSO and ethanol) at a concentration of 0.1% had no effect on $[Ca^{2+}]_i$ transients.

The pentapotassium salt of indo-1 and 4-Br A23187 were purchased from Molecular Probes Inc. (Eugene, OR).

RESULTS

Demonstration and validation of the experimental protocol

Intracellular [Ca^{2+}] in cardiac myocytes is regulated by a number of powerful transport systems, including Na-Ca exchange mechanisms of the sarcolemma and the mitochondria as well as Ca-ATPases located in the sarcoplasmic reticulum and sarcolemmal membrane (Bassani et al., 1992). The sarcolemmal Na-Ca exchanger and the SR Ca-ATPase, in particular, are capable of transporting large amounts of Ca^{2+} during a single cardiac contraction (Bers and Bridge, 1989). To study the binding properties of intracellular Ca^{2+} buffers, it is necessary to minimize Ca^{2+} movements caused by these mechanisms so that Ca^{2+} could equilibrate with the binding sites of interest.

Fig. 2 *A* shows the effect of inhibiting sarcolemmal Na-Ca exchange on stimulated $[Ca^{2+}]_i$ transients and illustrates the experimental paradigm used throughout these experiments. Initially, cells were superfused in a normal Tyrode's solution (145Na,2Ca) with a holding potential of −70 mV. Every 2 s, the cell was depolarized with a ramp pulse to −40 (to inactivate Na channels) just before a step depolarization to 0 mV for 100 ms to elicit a $[Ca^{2+}]_i$ transient. During these depolarizations, the $[Ca^{2+}]_i$ transient achieved a steady-state waveform that was characterized by reproducible resting and peak levels of $[Ca^{2+}]_i$. After a steady state was achieved in this superfusion solution, depolarizing pulses were terminated and the superfusion solution was rapidly switched for 10 s to a 145Na,2Ca solution containing 20 mM caffeine to deplete SR Ca^{2+} (not shown). Exposure to caffeine-containing solution was repeated to ensure that the SR was

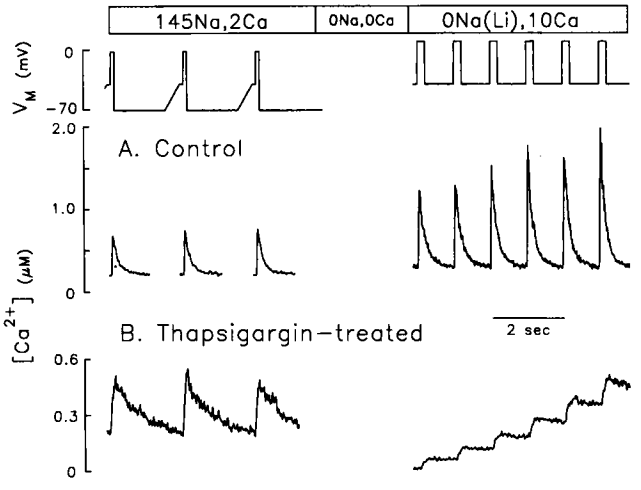

FIGURE 2 The effect of inhibiting Ca^{2+} removal mechanisms on depolarization-induced increases in $[Ca^{2+}]_i$. The top panel shows the solution protocol used in this and all other figures. Cells were initially superfused in a normal Tyrode's solution, followed by superfusion in Na-free solutions containing 0 and then 10 mM free Ca^{2+}. The second panel shows the voltage clamp protocols used in 145Na,2Ca and 0Na,10Ca solutions. (*A*) Control. This myocyte was exposed to vehicle (0.1% DMSO). (*B*) Thapsigargin-treated. A second myocyte was superfused with a normal Tyrode's solution containing 2.5 μM thapsigargin for 5 min before the solution and voltage clamp protocol shown. SR Ca^{2+} was depleted by two 10-s exposures to 20 mM caffeine in 145Na,2Ca solution after the $[Ca^{2+}]_i$ transients shown in the left panel but before the step-wise increases in $[Ca^{2+}]_i$ shown in the right panel.

largely depleted of releasable Ca^{2+}. During the second caffeine exposure, the superfusion solution was switched to a Na-free, Li-substituted, Ca-free solution (0Na,0Ca) to deplete the cell of Na^+. After 3–5 min, the superfusion solution was changed to a Na-free, Li-substituted, 10 mM $CaCl_2$-containing solution (0Na,10Ca), and the holding potential changed to −40 mV. Under these conditions, sarcolemmal Na-Ca exchange should be abolished because intracellular and extracellular solutions are both Na-free. This assumption was verified in some cells by monitoring $[Ca^{2+}]_i$ for periods of up to 1 min after switching to 0Na,10Ca superfusion solution. In the absence of depolarizing voltage clamp pulses, resting $[Ca^{2+}]_i$ increased very little or not at all (not shown). Thus, this solution protocol effectively depletes the cell of Na^+ and prevents Na-Ca exchange.

During superfusion in 0Na,10Ca solution, 200 ms depolarizing pulses to +10 mV at 1 Hz elicited $[Ca^{2+}]_i$ transients whose amplitude became steadily larger with each clamp pulse (Fig. 2 *A*, *right* panel). Basal $[Ca^{2+}]_i$ increased only slightly until, eventually, spontaneous $[Ca^{2+}]_i$ transients were observed (not shown). Thus, in Na-free superfusion solution, cellular Ca^{2+} loading increased with each depolarization. This is consistent with the idea that the sarcolemmal Na-Ca exchanger is the major pathway for Ca^{2+} efflux from the cell and that, in the absence of Na-Ca exchange, Ca^{2+} that enters during each depolarization cannot be removed before the next stimulated $[Ca^{2+}]_i$ transient. Another noteworthy point is that the rate of decline of the $[Ca^{2+}]_i$ transients was not much slower than that observed when the cell was in 145Na,2Ca solution. This may reflect, in part, the larger size of the $[Ca^{2+}]_i$ transients (Berlin et al., 1990; Bers and Berlin, 1994), but it also points out that SR Ca^{2+} uptake is the major pathway for removal of Ca^{2+} from the cytosol during a transient in rat ventricle (Bers et al., 1990; Bassani et al., 1994).

Fig. 2 *B* shows a similar experiment carried out in a myocyte that had been exposed to 2.5 μM thapsigargin for 5 min during superfusion in 145Na,2Ca solution. At this concentration, thapsigargin is reported to irreversibly block Ca^{2+} sequestration into the SR (Kirby et al., 1992; Bassani et al., 1993). Depolarizing pulses elicited much smaller $[Ca^{2+}]_i$ transients than in untreated myocytes. The first exposure to 20 mM caffeine-containing solution released any Ca^{2+} remaining in the SR. Subsequent caffeine exposures, even with continued depolarizations, did not produce a large increase in $[Ca^{2+}]_i$ (not shown). This indicates that releasable Ca^{2+} in the SR was depleted by the first caffeine exposure and that, subsequently, reaccumulation was blocked by thapsigargin. The marked slowing of the decline in $[Ca^{2+}]_i$ during stimulated transients in this thapsigargin-treated cell is also consistent with inhibition of SR Ca^{2+} sequestration.

After caffeine application, this cell was superfused in 0Na,0Ca and then 0Na,10Ca solution as described above. Depolarizations from −40 to +10 mV during superfusion in 0Na,10Ca solution elicited step-wise increases in $[Ca^{2+}]_i$ that showed only a very slow decrease in $[Ca^{2+}]_i$ between depolarizations. Thus, blockade of Na-Ca exchange and SR Ca-ATPase largely abolishes rapid phasic changes in $[Ca^{2+}]_i$. Furthermore, changes in $[Ca^{2+}]_i$ under these conditions are slow enough so that buffers that bind a significant amount of Ca^{2+} during a single $[Ca^{2+}]_i$ transient are likely to be in equilibrium with $[Ca^{2+}]_i$.

Fig. 3 shows this same protocol in three other thapsigargin-treated cells that were superfused in 0Na,10Ca solution and depolarized from −40 to +10 mV for 200 ms at 1 Hz. As in Fig. 2 *B*, depolarizations led to step increases in $[Ca^{2+}]_i$ that went into the micromolar range, similar to the peak level of $[Ca^{2+}]_i$ observed during a stimulated $[Ca^{2+}]_i$ transient. In the absence of SR Ca^{2+} release and sarcolemmal Na-Ca exchange, the only source for Ca^{2+} that increased $[Ca^{2+}]_i$ was the Ca current, shown in Fig. 3 *A* (*bottom* panel) as an extracellular Ca-sensitive difference current. It is also apparent that $[Ca^{2+}]_i$ decreased slowly between depolarizations when $[Ca^{2+}]_i$ became elevated. The half-time for this decline of $[Ca^{2+}]_i$ was 5–10 s as evidenced by the slow decline of $[Ca^{2+}]_i$ after cessation of depolarizing pulses in Fig. 3 *B*. This decline of $[Ca^{2+}]_i$ could be caused by residual Ca^{2+} transport out of the myoplasm or could reflect slow buffering of Ca^{2+}.

To determine whether residual SR Ca^{2+} transport was responsible for the decline of $[Ca^{2+}]_i$, 145Na,2Ca solution containing 20 mM caffeine was rapidly applied to the myocyte in Fig. 3 *B* after the last depolarization. Caffeine application did produce a small increase in $[Ca^{2+}]_i$ from 770

nM (extrapolated from the rate of $[Ca^{2+}]_i$ decline) to 880 nM. However, as pointed out in the Discussion, this increase in $[Ca^{2+}]_i$ represents a very small fraction of total Ca^{2+} over 13 depolarizations and would only amount to a 3% error in calculation of total Ca^{2+} binding in the cytosol. These results do demonstrate, nonetheless, that some small residual Ca^{2+} uptake by the SR could be present, even though the rate of this uptake must be markedly slower than in thapsigargin-free cells. Thus, as a precaution, all cells used in the analysis of Ca^{2+} buffering were exposed to 20 mM caffeine after the train of depolarizing voltage clamp pulses increased $[Ca^{2+}]_i$. Cells showing large increases in $[Ca^{2+}]_i$ upon application of caffeine were excluded from further analysis.

Another possible mechanism for slow removal of Ca^{2+} from the cytosol is uptake by the mitochondria, particularly in the presence of prolonged elevation of $[Ca^{2+}]_i$ (Miyata et al., 1991; Bassani et al., 1992). The possibility that the slow decline of $[Ca^{2+}]_i$ was caused by mitochondrial uptake was tested as shown in Fig. 3 *C*. A myocyte treated with thapsigargin and superfused in Na-free solution, as in Fig. 3 *A*, produced a large increase in $[Ca^{2+}]_i$ in response to the train of depolarizing pulses from −40 to +10 mV (Control). At elevated $[Ca^{2+}]_i$, there was a slow decline in $[Ca^{2+}]_i$ between depolarizations. After these depolarizing pulses, caffeine was applied to ensure that the SR was depleted of releasable Ca^{2+} and the cell was superfused in 0Na,0Ca for an additional 5 min to ensure that cellular Na^+ and Ca^{2+} were depleted. The superfusion solution was then returned to a 0Na,10Ca solution that contained 5 μM "1799," a mitochondrial uncoupler (LaBelle and Racker, 1977). After 30-s exposure to "1799"-containing solution, depolarizations at 1 Hz again elicited step increases in $[Ca^{2+}]_i$ ("1799"). The increases in $[Ca^{2+}]_i$ resulting from each depolarization were smaller than those during the Control period. This probably represents the degree of run-down in the cell, as judged by the decrease in the size of the Ca current (not shown) and an increased cytosolic buffering capacity resulting from a higher cytosolic indo-1 concentration. More important, when $[Ca^{2+}]_i$ became elevated, $[Ca^{2+}]_i$ still showed a slow decrease between depolarizations. The inset of Fig. 3 *C* shows superimposed $[Ca^{2+}]_i$ traces that suggest, at similar $[Ca^{2+}]_i$, the rate of decline of $[Ca^{2+}]_i$ between depolarizations was similar in the presence or absence of "1799." Similar results were obtained in two additional experiments. These data suggest that mitochondrial uptake of Ca^{2+} was not the major mechanism in the slow decline of $[Ca^{2+}]_i$.

In summary, superfusion of thapsigargin-treated myocytes in 0Na,10Ca solution allows depolarizing pulse trains to produce step-wise increases in $[Ca^{2+}]_i$. However, a slow decline of $[Ca^{2+}]_i$ ($T_{1/2}$ > 5 s) can still be observed when $[Ca^{2+}]_i$ becomes elevated. Even so, the slow decline of $[Ca^{2+}]_i$ may

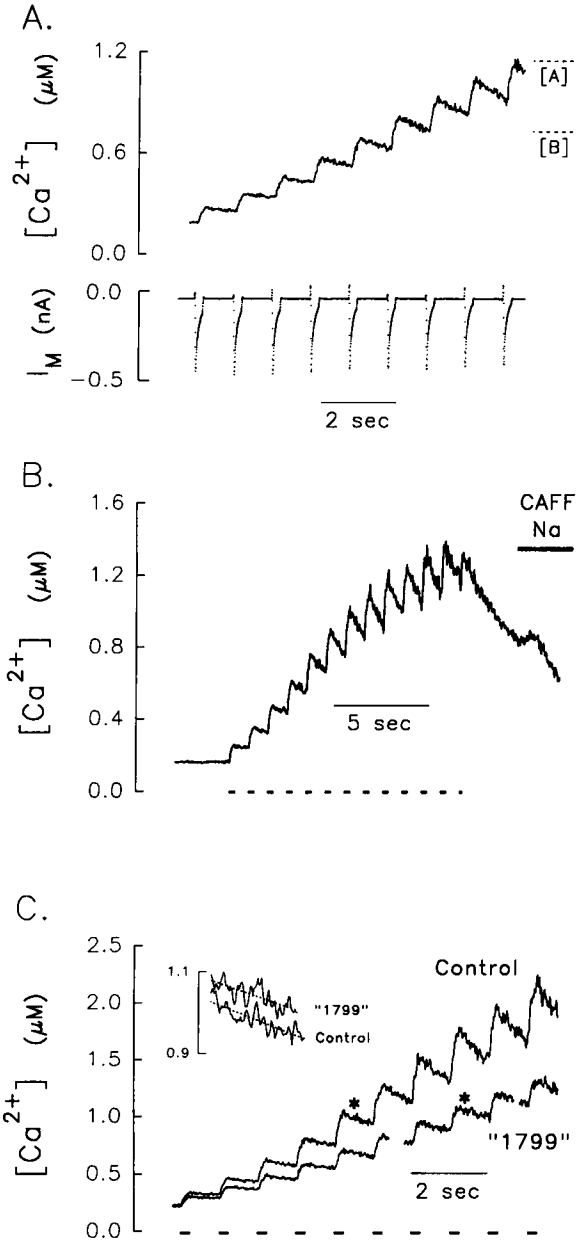

FIGURE 3 Characterization of elevated $[Ca^{2+}]_i$ in thapsigargin-treated myocytes. Different myocytes (*A–C*) were exposed to 10 μM thapsigargin for 3 min in 145Na,2Ca solution, followed by superfusion in 0Na,0Ca and 0Na,10Ca solutions. Depolarizations of 200 ms duration from −40 to +10 mV were produced at 1 Hz, as in Fig. 2 *B*. (*A*) $[Ca^{2+}]_i$ and Ca current. $[Ca^{2+}]_i$ (*top*) and Ca current (*bottom*) during the 1-Hz train of depolarizations is shown. Ca current is displayed as the extracellular Ca-sensitive difference current calculated by subtracting current measured during superfusion in 0Na,0Ca solution from that measured in 0Na,10Ca solution. Equilibrium $[Ca^{2+}]_i$ ([A]) was estimated by assuming that cytosolic Ca^{2+} buffering had the characteristics described in Fig. 5 plus the slow Ca^{2+} buffering described by Robertson et al. (1981) or ([B]) Hove-Madsen and Bers (1993) plus 50 μM indo-1 (see Discussion). (*B*) SR Ca^{2+} sequestration during superfusion in 0Na,10Ca solution. Another thapsigargin-treated myocyte was subjected to a train of 1-Hz depolarizations followed by rapid application of 20 mM caffeine in 145Na,2Ca solution to release any Ca^{2+} sequestered in the SR. (*C*) Effect of a mitochondrial uncoupler on changes in $[Ca^{2+}]_i$ during superfusion in 0Na,10Ca solution. This myocyte was exposed to 0Na,10Ca solution, first in the absence and then in the presence of 5 μM "1799," a mitochondrial uncoupler (see text for details). Slow decreases of $[Ca^{2+}]_i$ for the starred pulses are shown in greater detail in the inset. The dashed line at the bottom of *B* and *C* indicate the timing of depolarizations from −40 to +10 mV.

not prevent the estimation of fast Ca^{2+} buffering that would be important during a stimulated transient.

Analysis of cytosolic Ca^{2+} buffering

To accurately estimate cytosolic Ca^{2+} buffering characteristics, it is necessary to know two factors: (1) the change in $[Ca^{2+}]_i$, and (2) the total amount of Ca^{2+} that entered into the cytosolic space to produce that change in $[Ca^{2+}]_i$. These two variables were measured from changes in indo-1 fluorescence and the integral of the Ca current, respectively. An example of this procedure is shown in Fig. 4 with data taken from the same myocyte shown in Fig. 3 *A*. The Ca current (*top* panel) and $[Ca^{2+}]_i$ (*middle* panel) are shown at the time of the fourth depolarization from −40 to +10 mV during superfusion in 0Na,10Ca solution. Before the depolarization, $[Ca^{2+}]_i$ was slowly decreasing, and upon depolarization the rise in $[Ca^{2+}]_i$ was synchronous with the activation of inward current. Upon repolarization and current deactivation, the rise in $[Ca^{2+}]_i$ ceased and a slow decline in $[Ca^{2+}]_i$ continued but from a more elevated level. The middle panel of Fig. 4 also shows that the time course of integrated Ca current superimposed on the rise in $[Ca^{2+}]_i$. This result was consistent with the assumption that Ca current was the only source of Ca^{2+} under these conditions and suggested that Ca^{2+} influx rapidly equilibrated with cellular buffers.

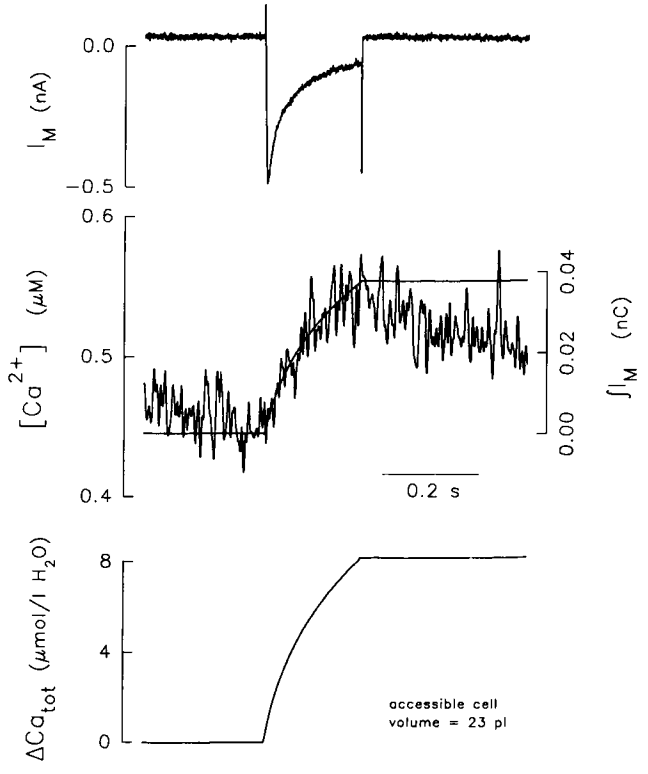

FIGURE 4 Correlation between Ca current and $[Ca^{2+}]_i$. The top panel shows the extracellular Ca-sensitive difference current for a depolarization from −40 to +10 mV. The middle panel shows $[Ca^{2+}]_i$ (noisy trace) and the integral of the Ca current. The bottom panel is the change in total cytosolic $[Ca^{2+}]$ calculated as moles of Ca influx via the Ca current divided by the accessible cytosolic volume.

The integral of the Ca current gives information on the total moles of Ca^{2+} that enter the cytosol; however, this value must be converted into units of mol/liter to calculate Ca^{2+} buffering characteristics. Thus, it is necessary to determine the cytosolic volume into which the Ca^{2+} influx is diluted. For this cell, accessible cellular volume (i.e., that portion of total cell volume not occupied by membrane-bound compartments such as mitochondria) was calculated to be 23 pl as described in Materials and Methods. Thus, 0.038 nC of charge carried during the Ca current translates into an increase of 8.2 μmol Ca^{2+}/l accessible cytosolic H_2O. This procedure applied to each voltage clamp pulse provides the information needed to determine cytosolic Ca^{2+} buffering, i.e., the change in $[Ca^{2+}]_i$ and the change in total Ca^{2+}.

The simplest expression that would be expected to describe cytosolic Ca^{2+} buffering over the physiological range of $[Ca^{2+}]_i$ is the traditional Michaelis-Menten relationship below:

$$[BCa] = \frac{[Ca^{2+}] * B_{max}}{K_D + [Ca^{2+}]}, \quad (2)$$

where K_D is the lumped dissociation constant for all buffers, B_{max} is the sum of the capacities of all the buffers, and [BCa] is the concentration of bound Ca^{2+} calculated as total Ca^{2+} minus free Ca^{2+}. However, the slow changes in $[Ca^{2+}]_i$ preclude the traditional methods for estimation of K_D and B_{max}. By focusing on fast Ca^{2+} buffering where the change in free $[Ca^{2+}]_i$ (d$[Ca^{2+}]$) parallels the change in total Ca^{2+} during a voltage clamp pulse (Fig. 4, *middle* panel), the change in bound Ca^{2+} (d[BCa]) is also known, and as long as the stepwise change of $[Ca^{2+}]_i$ with each depolarization is small, Eq. 2 can be differentiated with respect to Ca^{2+} so that

$$\frac{d[BCa]}{d[Ca^{2+}]} = \frac{B_{max} * K_D}{(K_D + [Ca^{2+}]_m)^2}, \quad (3)$$

where $[Ca^{2+}]_m$ is the mean level of $[Ca^{2+}]_i$ during a step increase in $[Ca^{2+}]_i$. Using this relationship, it is possible to estimate K_D and B_{max} using a nonlinear curve-fitting routine. Such a procedure was performed using the current and $[Ca^{2+}]_i$ data from the myocyte in Fig. 3 *A*. The change in $[Ca^{2+}]_i$ (d$[Ca^{2+}]$) was calculated as $[Ca^{2+}]_i$ after repolarization minus that just before the depolarization, and $[Ca^{2+}]_m$ was calculated as the average of $[Ca^{2+}]_i$ at these two time points. The integral of each Ca current was determined, and the change in total $[Ca^{2+}]$ was calculated for each depolarization, as in Fig. 4. The change in bound $[Ca^{2+}]$ (d[BCa]) was then calculated as change in total $[Ca^{2+}]$ minus the d$[Ca^{2+}]$. Fig. 5 shows the results of these calculations. As predicted by Eq. 3, d[BCa]/d$[Ca^{2+}]$ became smaller as $[Ca^{2+}]_i$ was elevated, a reflection of the increased saturation of Ca^{2+} buffers at higher $[Ca^{2+}]_i$. The solid curve was fit using Eq. 3 as the input function and the predicted K_D was 0.89 μM and B_{max} was 178 μM. Data from five cells were used to obtain an estimate of the K_D for cytosolic Ca^{2+} buffers equal to 0.63 ± 0.07 μM (mean ± SEM) and the total buffering capacity of the cytosol equal to 162 ± 15 μmol/l cell H_2O (Table 1).

The values of K_D and B_{max} for total cytosolic buffering includes Ca^{2+} binding to intrinsic cellular buffers as well as

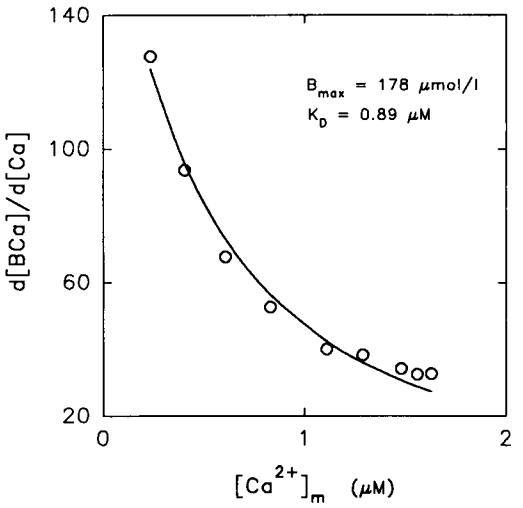

FIGURE 5 Calculation of total cytosolic Ca^{2+} buffers. The change in bound cytosolic Ca divided by the change in $[Ca^{2+}]_i$ (d[BCa]/d[Ca]) for each depolarization during the 1-Hz train of depolarizations is plotted as a function of $[Ca^{2+}]_m$, the mean $[Ca^{2+}]_i$ (see text for details). The curve was best-fit by a nonlinear least-squares routine using Eq. 3 and the K_D and B_{max} shown.

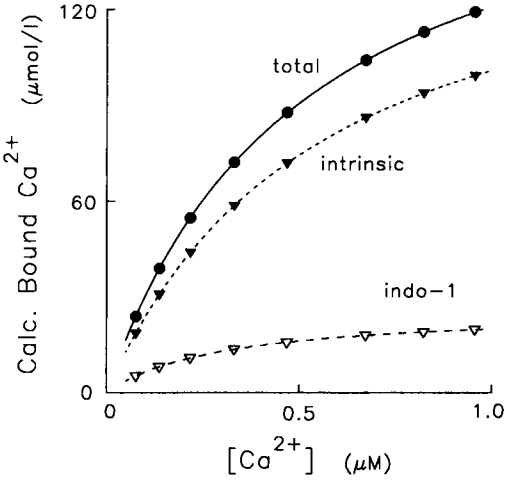

FIGURE 6 Estimation of intrinsic cytosolic Ca^{2+} buffers. Ca^{2+} bound to total cytosolic buffers and indo-1 was estimated with the following buffer parameters (from Table 1): total cytosolic K_D = 0.50 μM, B_{max} = 182 μmol/l (——); indo-1 K_D = 0.33 μM and B_{max} = 26 μmol/l (– – –). The binding isotherm for intrinsic buffers (- - - -) was calculated as Ca^{2+} bound to total cytosolic buffers minus Ca^{2+} bound to indo-1. Parameters for intrinsic buffers in this cell are K_D = 0.55 μM and B_{max} = 158 μmol/l.

Ca^{2+} binding to indo-1. Thus, to determine the properties of the intrinsic Ca^{2+} buffers, it is necessary to account for Ca^{2+} binding to indo-1 and subtract it from the total Ca^{2+} bound within the cytosol. To estimate Ca^{2+} bound to indo-1, cytosolic indo-1 concentration was determined by comparing the fluorescence intensity of the cell at the isosbestic wavelength against the fluorescence intensity of an indo-1 solution in a thin capillary. Cytosolic indo-1 concentration was then calculated using Eq. 1 (see Materials and Methods for a full description). The results of these calculations are shown in Table 1 with the average concentration being equal to 44 ± 5 μM. Ca^{2+} binding to indo-1 was then estimated assuming a K_D of 0.33 μM (Fig. 1 *A*).

Intrinsic Ca^{2+} buffering was calculated by subtracting the Ca^{2+} calculated to be bound to indo-1 from the total Ca^{2+} estimated to be bound to cytosolic buffers using the K_D and B_{max} calculated for total cytosolic buffering. Fig. 6 shows an example of one such calculation where B_{max} and K_D determined in a myocyte were used with Eq. 2 to calculate the total bound Ca^{2+} in the cytosol (total) and the calculated cellular indo-1 concentration was used to calculate Ca^{2+} bound to indo-1 (indo-1). The difference between these two quantities was assumed to represent Ca^{2+} binding to intrinsic cytosolic buffers, and K_D and B_{max} were calculated for this intrinsic Ca^{2+} binding. These data, summarized in Table 1, show that the Ca^{2+} binding capacity of the cytosol was 123 ± 18 μmol/l with a K_D of 0.96 ± 0.18 μM.

Fig. 3 C pointed out that mitochondrial uptake of Ca^{2+} did not appear to be a major mechanism for Ca^{2+} transport in these experiments. To test this conclusion, the protocol to measure intrinsic cytosolic Ca^{2+} buffering was repeated twice in the same cell, once under control conditions and then again in the presence of the mitochondrial uncoupler, "1799" (Table 1). The calculated values of K_D and B_{max} for intrinsic Ca^{2+} buffering were not significantly different in the absence and presence of "1799." These data confirmed that the mitochondria did not have a major role in Ca^{2+} movements under the conditions of these experiments.

Another way to view these data is to consider how much Ca^{2+} would be involved in a $[Ca^{2+}]_i$ transient that raises $[Ca^{2+}]_i$ from 100 nM to a peak of 1 μM. The parameters for intrinsic Ca^{2+} buffers calculated above predict that such a transient would add 51 μmol/l Ca^{2+} to the cytosol. Given that the Ca^{2+} influx during the Ca current is approximately 8 μmol/l (Fig. 4), 43 μmol/l or 84% of total Ca^{2+} would be released from the SR, consistent with Fig. 2 and previous reports that rat ventricular myocytes are largely dependent on SR Ca^{2+} release for stimulated transients (Cannell et al., 1987; Bers et al., 1990).

DISCUSSION

The present study examined Ca^{2+} buffering in the cytosolic space of rat cardiac ventricular myocytes. Many potential Ca^{2+} buffering sites have been identified in cardiac myocytes, including fixed buffer sites on contractile proteins such as myosin and troponin (Solaro et al., 1974; Robertson et al., 1981), transport proteins such as Ca-ATPases and membrane phospholipids (Fabiato, 1983). Potentially mobile buffers including ATP, phosphocreatine, and calmodulin can also contribute to cytosolic Ca^{2+} buffering (Fabiato, 1983). These sites are present in high concentration and, given the tight regulation of $[Ca^{2+}]_i$ by the cell, could be very important in modulating Ca^{2+}-dependent processes within the cell. The Ca^{2+}-binding properties of these buffers have been examined in vitro, in muscle homogenates (Pierce et al., 1985), in chemically skinned fibers (Pan and Solaro, 1987), and in

permeabilized myocytes (Hove-Madsen and Bers, 1993). Changes in myoplasmic Ca content during the contraction cycle have also been studied by electron microprobe analysis (Moravec and Bond, 1991; Wendt-Gallitelli and Isenberg, 1991), but the extent of Ca^{2+} buffering in these two studies varied widely (see below). Thus, the goal of this study was to estimate Ca^{2+} binding in the cytosol of voltage-clamped myocytes so that Ca^{2+} buffering, which plays a role in controlling changes in $[Ca^{2+}]_i$ during stimulated contractions, could be determined.

Our methods did not allow us to distinguish between the properties of individual Ca^{2+} binding species, so we analyzed Ca^{2+} buffering under the assumption that all buffers behaved as a single lumped species that had a one-to-one binding relationship with Ca^{2+}. The binding properties of very low affinity buffers also could not be determined in these experiments. As such, an unique solution to the Ca^{2+} buffering properties of the cytosol was not possible. Instead, the present experiments achieved a description of buffering properties over a range of $[Ca^{2+}]_i$ that included those levels of $[Ca^{2+}]_i$ observed during a transient. Buffers that bind significant quantities of Ca^{2+} during the $[Ca^{2+}]_i$ transient should have been well described. Given these limitations, the intrinsic buffers in the cytosol were described by a K_D of 0.96 $\pm$ 0.18 μM with a binding capacity of 123 $\pm$ 18 μmol/l cell H_2O.

The $[Ca^{2+}]_i$ reported in this paper were estimated from changes in indo-1 fluorescence using the calibration parameters R_{min}, R_{max}, and β determined in myocytes, but a K_D determined under in vitro conditions. It is worth examining what effect changes in indo-1 Ca^{2+} affinity would have on the calculated buffer parameters because several papers suggest that Ca^{2+} affinity of these indicators is decreased in the cell (Hove-Madsen and Bers, 1992; Backx and ter Keurs, 1993) and by protein binding (see Fig. 1 and Konishi et al., 1988). Table 1 shows such a calculation for the same myocyte used in Figs. 3 *A*, 4, and 5 where the K_D of indo-1 for Ca^{2+} has been increased fourfold (Konishi et al., 1988; Hove-Madsen and Bers, 1992). It is quite clear that the apparent affinity of the lumped buffer also decreases fourfold but B_{max} is relatively unchanged. Thus, regardless of the affinity of indo-1 for Ca^{2+}, the buffering capacity of the cytosol will be accurately determined; however, the $[Ca^{2+}]_i$ and the buffer K_D will be scaled with the presumed Ca^{2+} affinity of the indicator.

Determination of cytosolic Ca buffering

The experimental paradigm to determine these buffer parameters relied upon the quantitation of exchangeable Ca content within the cytosolic space. This was accomplished by inhibiting Ca^{2+} removal processes and measuring Ca^{2+} influx into the cell. Measuring Ca^{2+} influx was very straightforward because the integral of the Ca current during superfusion of Na-free solutions reflects Ca^{2+} influx into the cell in the absence of Na-Ca exchange. Furthermore, Ca^{2+} release from the SR was prevented by inhibiting SR Ca^{2+} uptake with thapsigargin and then depleting intracellular Ca^{2+} stores by repeated exposure to caffeine. This procedure has been shown to effectively deplete SR Ca^{2+} release and prevent Ca^{2+} uptake (Bassani et al., 1993; Janczewski and Lakatta, 1993). Under these conditions, Ca current should represent all Ca^{2+} coming into the cytosol during a depolarization. Determining that Ca^{2+} removal processes were inhibited, on the other hand, was more difficult.

The processes thought to be particularly important for the rapid removal of cytosolic Ca^{2+} are the sarcolemmal Na-Ca exchange mechanism and the Ca-ATPase of the SR. These processes were blocked with the use of Na-free solutions and thapsigargin, respectively. Na-free superfusion solution alone had only a small effect on the rate of removal of Ca^{2+} during a transient. Thapsigargin, on the other hand, produced a much greater slowing of the decay of the $[Ca^{2+}]_i$ transient, consistent with the finding that rat myocytes rely largely upon the SR to sequester Ca^{2+} after a transient (Bers et al., 1990; Bassani et al., 1994). These two maneuvers together produced a profound slowing of Ca^{2+} removal from the cytosol. This is evidenced by the step increases of $[Ca^{2+}]_i$ in thapsigargin-treated cells that were superfused in 0Na,10Ca solution and a half-time for the slow decrease of $[Ca^{2+}]_i$ that was 5–10 s, i.e., approximately 50- to 100-fold slower than under control conditions. Thus, Na-Ca exchange and SR Ca^{2+} sequestration appear to account for almost all of the rapid removal of Ca^{2+} in rat ventricular myocytes (Bassani et al., 1994).

The mechanism underlying the slow decrease in elevated $[Ca^{2+}]_i$ during superfusion of thapsigargin-treated cells in Na-free solution was also examined. One possibility examined was that some residual Ca^{2+} uptake by the SR remained after thapsigargin treatment. After Ca^{2+} loading of the myocytes, 20 mM caffeine was briefly applied to release any Ca^{2+} sequestered in the SR. As shown in Fig. 3 *B*, only a small change in $[Ca^{2+}]_i$ occurred as a result of this caffeine application. Using the parameters for total Ca^{2+} buffering in Table 1, the total amount of Ca^{2+} calculated to be released by caffeine was 4 μmol/l. If the amount released is due entirely to Ca^{2+} uptake during superfusion in 0Na,10Ca solution, this suggests that the calculated B_{max} of 162 μmol/l was underestimated by approximately 3%, a relatively small error.

The possibility that the slow decline in $[Ca^{2+}]_i$ was caused by mitochondrial uptake was also tested by Ca^{2+} loading cells in the presence of "1799," a nonfluorescent proton ionophore that uncouples oxidative phosphorylation in the mitochondria (LaBelle and Racker, 1977). By dissipating the proton gradient across the inner mitochondrial membrane, 1799 can prevent Ca^{2+} uptake into the mitochondria. Even in the presence of this drug, the slow decline of $[Ca^{2+}]_i$ was still observed (Fig. 3 *C*). Furthermore, cytosolic Ca^{2+} buffering parameters estimated in the presence and absence of this mitochondrial uncoupler were only slightly different (Table 1). These data suggest that mitochondrial Ca^{2+} uptake is not the major cause of the slow decline of $[Ca^{2+}]_i$. Additional mechanisms could also explain the slow decline in

$[Ca^{2+}]_i$. Ca^{2+} efflux via the sarcolemmal Ca-ATPase is one such mechanism; however, this ATPase appears to remove cytosolic Ca^{2+} very slowly in cardiac myocytes (Bassani et al., 1992). Even so, we cannot completely rule out the possibility that some Ca^{2+} transport occurred during the slow decline of $[Ca^{2+}]_i$.

Another possibility is that Ca^{2+} binding to slow buffers such as the Ca/Mg sites of troponin and myosin (see below) could account for slow changes in $[Ca^{2+}]_i$ (Konishi and Berlin, 1993). Ca^{2+} binding at these sites is likely to occur only after the displacement of bound Mg^{2+}, a process that may occur with rate constants of less than 1 s^{-1} (Robertson et al., 1981; Konishi and Berlin, 1993). At this time, identification of the mechanism responsible for slow changes in $[Ca^{2+}]_i$ is not possible.

The presence of slow changes in $[Ca^{2+}]_i$ between depolarizations prevented us from analyzing total cytosolic buffering, i.e., fast and slow Ca buffer species, simply by summing the integrals of the Ca currents and then calculating B_{max} and K_D based upon the $[Ca^{2+}]_i$. Instead, our analysis of Ca^{2+} buffering was limited to fast Ca buffers. These buffers, such as the Ca-specific site of troponin and the binding sites on calmodulin, are thought to be largely free of bound Mg^{2+} at physiological resting $[Ca^{2+}]_i$. Increases in $[Ca^{2+}]_i$ bring about increased binding at these sites limited only by the association (i.e., diffusion-limited) and dissociation rate constants for Ca^{2+}. Thus, binding of Ca^{2+} to fast buffers is thought to follow closely the waveform of changes in $[Ca^{2+}]_i$ (Robertson et al., 1981; Konishi and Berlin, 1993). These fast binding sites should be important, therefore, in buffering $[Ca^{2+}]_i$ during the rapid changes in $[Ca^{2+}]_i$ during a transient.

Comparison with published values

Fig. 7 *A* shows cytosolic Ca^{2+} binding calculated from the present experiments (single myocyte), those of Hove-Madsen and Bers (1993), and presumed properties of known cellular Ca^{2+} buffers (Fabiato, 1983) as a function of $[Ca^{2+}]$. It was somewhat surprising that the present results agree well with the tabulation of known Ca^{2+} buffers proposed by Fabiato (1983), because additional Ca^{2+} binding sites are expected in the cytosol (see below) and the Ca^{2+} binding to troponin C and the SR Ca-ATPase were probably underestimated by Fabiato (Bers, 1991; Wier et al., 1994).

Neither the present experiments nor those of Hove-Madsen and Bers (1993) experimentally determined the amount of Ca^{2+} bound in the cytosol. Rather, the change in bound Ca^{2+} was measured as a function of $[Ca^{2+}]$. A comparison of the change in bound Ca (see Fig. 7 *B*) shows that Ca^{2+} buffering in the present experiments is approximately half of that measured with digitonin-permeabilized myocytes (Hove-Madsen and Bers, 1993). Possible explanations for this difference include: 1) Ca^{2+} binding to slow Ca buffers, 2) overestimation of Ca^{2+} buffering by Hove-Madsen and Bers (1993), and 3) underestimation of buffering in the present experiments.

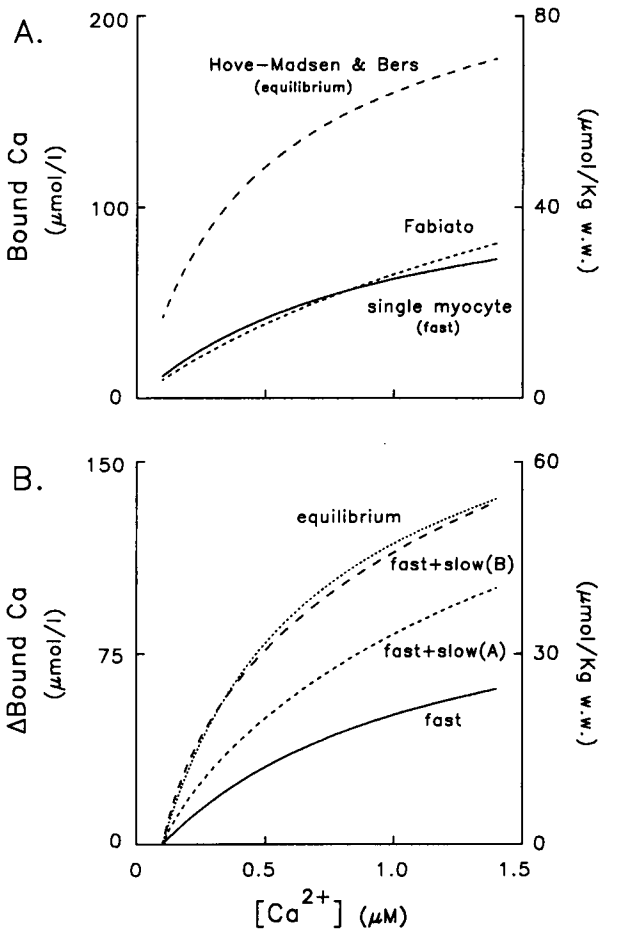

FIGURE 7 Comparison of intrinsic cytosolic Ca^{2+} buffers with published data. (*A*) Calculated bound Ca^{2+} is plotted against $[Ca^{2+}]$ using the mean K_D and B_{max} for intrinsic cytosolic buffering in Table 1 (single myocyte), K_D and B_{max} values from Hove-Madsen and Bers (1993), and the sum of cytosolic Ca buffers listed in Table 2 of Fabiato (1983). (*B*) Calculated cytosolic buffers and the effect of slow Ca buffers. The change in bound Ca^{2+} from an initial level at 100 nM $[Ca^{2+}]$ was calculated for the present data (fast) and that of Hove-Madsen and Bers (1993) (equilibrium). The curve labeled "fast + slow(A)" is that calculated by summing the change in Ca^{2+} binding predicted by the present data with that predicted for equilibrium Ca^{2+} binding to the Ca/Mg sites of troponin and myosin. The Ca^{2+} and Mg^{2+} affinities of the Ca/Mg sites are taken from Robertson et al. (1981). Myosin and troponin concentrations are taken from Fabiato (1983) assuming that myosin and troponin exist in a 1:1 ratio in the cytosol and that the molar ratio of Ca/Mg sites on cardiac troponin to Ca-specific sites is 2:1 (Robertson et al., 1981). The curve labeled "fast+slow(B)" is the same as "fast+slow(A)" except that the Mg^{2+} affinity of the Ca/Mg sites on troponin have been increased 10-fold.

Ca^{2+} binding to slow buffers is a reasonable possibility because Hove-Madsen and Bers (1993) measured equilibrium Ca^{2+} binding over many minutes, whereas only fast Ca^{2+} buffering over 200 ms was assessed in the present analysis. The potential contribution of known slow Ca buffers to equilibrium Ca^{2+} binding can be estimated by calculating Ca^{2+} binding to the Ca/Mg sites of troponin C and myosin. The Ca^{2+} and Mg^{2+} binding properties were taken from Robertson et al. (1981) and the protein concentrations from Fabiato (1983). For 1 mM Mg^{2+} (as in the electrode

solution), the change in the equilibrium Ca^{2+} binding to these slow buffers was calculated and added to the fast buffering measured in the present experiments (fast+slow(A) in Fig. 7 *B*). This calculation indicates that Ca^{2+} binding to Ca/Mg sites on troponin C and myosin could contribute appreciably to equilibrium Ca^{2+} buffering.

The present data, however, suggest that equilibrium Ca^{2+} buffering would be greater than that predicted by including Ca^{2+} binding to these slow buffers. Equilibrium $[Ca^{2+}]_i$ at the end of the trace in Fig. 3 *A* can be estimated if these Ca^{2+} buffering characteristics of the cytosol are assumed. Integration of the Ca currents elicited by the nine depolarizations in Fig. 3 *A* gives an increase in total Ca^{2+} of 88.2 μM. With only the fast Ca^{2+} buffering measured in the present experiments (Table 1), $[Ca^{2+}]_i$ should have increased to 1.75 μM (well off-scale in Fig. 3 *A*). With inclusion of the Ca/Mg sites of troponin C and myosin discussed above, $[Ca^{2+}]_i$ should have increased to 1.15 μM (shown as [A] in Fig. 3 *A*). It is clear, however, that $[Ca^{2+}]_i$ is falling below this level by the end of the trace. Thus, including Ca^{2+} binding to these slow buffers does not adequately predict the equilibrium level of $[Ca^{2+}]_i$.

If the Ca^{2+} buffering characteristics of Hove-Madsen and Bers (1993) are used in this calculation (plus 50 μM indo-1 in this cell), the predicted $[Ca^{2+}]_i$ after nine depolarizations would be 0.73 μM (shown as [B] in Fig. 3 *A*), well below the observed $[Ca^{2+}]_i$. Thus, the increased equilibrium Ca^{2+} buffering predicted by Hove-Madsen and Bers (1993) would also seem to be consistent with the present data.

This additional Ca^{2+} buffering could still be attributable to slow buffers. The Ca^{2+} affinities of troponin C and myosin are greatly affected by a number of factors, including their association with other proteins (Zot and Potter, 1987). For example, a 10-fold increase in the Mg^{2+} affinity of the Ca/Mg sites of troponin C (similar to that induced by phosphorylation of troponin T; Jahnke and Heilmeyer, 1980) would increase Ca^{2+} binding to slow buffers enough that the resulting curve is close to the data of Hove-Madsen and Bers (see fast+slow(B) in Fig. 7 *B*). Alternatively, additional slow Ca/Mg buffers such as the Mg^{2+}-sensitive Ca^{2+} binding sites on the inner sarcolemmal surface (Frankis and Lindenmayer, 1984; Bers et al., 1986) could contribute substantially to equilibrium Ca^{2+} binding (Hove-Madsen and Bers, 1993).

The data of Hove-Madsen and Bers (1993) might have overestimated equilibrium cytosolic buffering because Ca^{2+} binding to the external surface of the permeabilized myocytes would be included in their calculations. However, Ca^{2+}-binding phospholipids appear to be asymmetrically distributed to the inner sarcolemmal surface (Post et al., 1988) so that this error is likely to be small.

The present experiments could have underestimated cytosolic buffering for several reasons. Thapsigargin may greatly reduce Ca^{2+} binding to the SR Ca-ATPase (Sagara and Inesi, 1991). In addition, residual Ca^{2+} transport may still be present (see above). Finally, dialysis of mobile buffers could have occurred between the cell and patch electrode. However, in the one myocyte where estimation of cytosolic Ca^{2+} buffers was repeated after several minutes, no significant change in intrinsic buffering capacity was observed (Table 1). This indicates that, on the time-scale of these experiments, mobile buffers do not constitute a large fraction of total buffer capacity. Measurements in bovine chromaffin cells also suggest that very little of the cytosolic Ca^{2+} buffering capacity is highly mobile (Zhou and Neher, 1993).

Thus, after accounting for methodological and analytical differences, several reports are in reasonable agreement with regard to cytosolic Ca^{2+} buffering in cardiac myocytes (Fabiato, 1983; Pierce et al., 1985; Pan and Solaro, 1987; Hove-Madsen and Bers, 1993; Balke et al., 1994). However, one study using electron microprobe analysis (Wendt-Gallitelli and Isenberg, 1991) estimated fast cytosolic Ca^{2+} buffering 10 times larger than the present study. On the other hand, much smaller changes of myoplasmic Ca^{2+} during a twitch were reported by Moravec and Bond (1991) using similar methods. There is no obvious explanation for the large discrepancy in these two papers. Even so, the reported changes in SR Ca content (Moravec and Bond, 1991; Wendt-Gallitelli and Isenberg, 1991) are consistent with the predictions made from the present cytosolic buffering data. Thus, comparison with published reports suggests that the present data yield a reasonable estimate of fast Ca^{2+} buffering in the cytosol.

Importance of Ca buffering in determining the Ca fluxes in rat myocytes

Fig. 4 shows that a Ca current that produces a increment in total cytosolic $[Ca^{2+}]$ of 8 μmol/l yields an increase in $[Ca^{2+}]_i$ of less than 100 nM. This clearly makes the point that only 1% of Ca^{2+} in the cytosol remains unbound. The other 99% is rapidly complexed with any of the variety of potential buffers. The properties of these Ca buffers may be the single most important determinant of the magnitude of $[Ca^{2+}]_i$ changes during a transient. Thus, maneuvers that alter cytosolic buffering capacity such as loading high affinity Ca indicators, including fura-2 or indo-1, may have significant effects on any Ca^{2+}-dependent process under study (Berlin and Konishi, 1993; Balke et al., 1994).

Fig. 2 *A* shows that the amplitude of the $[Ca^{2+}]_i$ transient can exceed 1 μM during superfusion in Na-free solution. The binding parameters estimated for cytosolic buffering predict that such a transient requires at least 50 μmol of Ca^{2+} per liter cell H_2O be added to the cytosol to achieve these levels of $[Ca^{2+}]_i$. Given that the Ca current in Fig. 4 is typical for these experiments, only 8 μmol/l is due to Ca^{2+} influx across the sarcolemma. The remaining Ca^{2+}, over 80% of the total, appears to come from SR release, consistent with previous estimates (Cannell et al., 1987; Bers et al., 1990). Because peak Ca^{2+} is reached in approximately 25–35 ms under these conditions (Konishi and Berlin, 1993), the peak rate of release must be at least 1.5 mmol/l/s. In fact, this is likely an underestimate because the peak rate of release must occur well before peak $[Ca^{2+}]_i$ is observed. This release rate,

similar to that recently reported during stimulated $[Ca^{2+}]_i$ transients (Wier et al., 1994) is several times lower than the peak release rate in skeletal muscle (Baylor et al., 1983; Melzer et al., 1987). Even so, this is consistent with the fact that severalfold more $[Ca^{2+}]_i$ is involved in a skeletal muscle Ca^{2+} transient than appears to be involved in a cardiac muscle $[Ca^{2+}]_i$ transient, based on the data presented in this paper.

The authors wish to thank Trang D. Le for excellent technical assistance. This work was supported by grants from the National Institutes of Health to J. R. Berlin (HL-43712) and D. M. Bers (HL-30077).

REFERENCES

Backx, P. H., and H. E. D. J. ter Keurs. 1993. Fluorescent properties of rat cardiac trabeculae microinjected with fura-2 salt. *Am. J. Physiol.* 264: H1098–H1110.

Balke, C. W., T. E. Egan, and W. G. Wier. 1994. Processes that remove calcium from the cytoplasm during excitation-contraction coupling in intact rat heart cells. *J. Physiol.* 474:447–462.

Bassani, R. A., J. W. M. Bassani, and D. M. Bers. 1992. Mitochondrial and sarcolemmal Ca^{2+} transport reduce $[Ca^{2+}]_i$ during caffeine contractures in rabbit cardiac myocytes. *J. Physiol.* 453:591–608.

Bassani, J. W. M., R. A. Bassani, and D. M. Bers. 1993. Twitch-dependent SR Ca accumulation and release in rabbit ventricular myocytes. *Am. J. Physiol.* 265:C533–C540.

Bassani, J. W. M., R. A. Bassani, and D. M. Bers. 1994. Relaxation in rabbit and rat cardiac cells: species-dependent differences in cellular mechanisms. *J. Physiol.* 476:279–293.

Baylor, S. M., W. K. Chandler, and M. W. Marshall. 1983. Sarcoplasmic reticulum calcium release in frog skeletal muscle fibres estimated from arsenazo III calcium transients. *J. Physiol.* 344:625–666.

Berlin, J. R., J. W. M. Bassani, and D. M. Bers. 1994. Intrinsic cytosolic calcium buffering in single rat cardiac myocytes. *Biophys. J.* 66:92*a*. (Abstr.)

Berlin, J. R., D. M. Bers, and W. J. Lederer. 1990. Extracellular Na dependent and independent decay of the $[Ca]_i$ transient in rat cardiac myocytes. *Biophys. J.* 57:177*a*. (Abstr.)

Berlin, J. R., and M. Konishi. 1993. Ca^{2+} transients in cardiac myocytes measured with high and low affinity Ca^{2+} indicators. *Biophys. J.* 65: 1632–1647.

Bers, D. M. 1991. Excitation-Contraction Coupling and Cardiac Contractile Force. Kluwer Academic Publishers, Norwell, MA. 258 pp.

Bers, D. M., L.-A. H. Allen, and Y. Kim. 1986. Calcium binding to cardiac sarcolemmal vesicles: potential role as a modifier of contraction. *Am. J. Physiol.* 251:C861–C871.

Bers, D. M., and J. R. Berlin. 1994. The kinetics for $[Ca]_i$ decline in cardiac myocytes depends importantly on peak $[Ca]_i$. *Am. J. Physiol.* In press.

Bers, D. M., and J. H. B. Bridge. 1989. Relaxation of rabbit ventricular muscle by Na-Ca exchange and sarcoplasmic reticulum calcium pump. *Circ. Res.* 65:334–342.

Bers, D. M., W. J. Lederer, and J. R. Berlin. 1990. Intracellular Ca transients in rat cardiac myocytes: role of Na-Ca exchange in excitation-contraction coupling. *Am. J. Physiol.* 258:C944–C954.

Blatter, L. A., and W. G. Wier. 1990. Intracellular diffusion, binding and compartmentalization of the fluorescent calcium indicators indo-1 and fura-2. *Biophys. J.* 58:1491–1499.

Borzak, S., R. A. Kelly, B. K. Krämer, Y. Matoba, J. D. Marsh, and M. Reers. 1990. In situ calibration of fura-2 and BCECF fluorescence in adult rat ventricular myocytes. *Am. J. Physiol.* 259:H973–H981.

Cannell, M. B., J. R. Berlin, and W. J. Lederer. 1987. Effect of membrane potential changes on the calcium transient in single rat cardiac muscle cells. *Science.* 238:1419–1423.

Cannell, M. B., and W. J. Lederer. 1986. A novel experimental chamber for single-cell voltage-clamp and patch-clamp applications with low electrical noise and excellent temperature and flow control. *Pflügers Arch.* 406:536–539.

Fabiato, A. 1983. Calcium-induced release of calcium from the cardiac sarcoplasmic reticulum. *Am. J. Physiol.* 245:C1–C14.

Fabiato, A., and A. Fabiato. 1979. Calculator programs for computing the composition of the solutions containing multiple metals and ligands used for experiments in skinned muscle cells. *J. Physiol. (Paris).* 75:463–505.

Frankis, M. B., and G. E. Lindenmayer. 1984. Sodium-sensitive calcium binding to sarcolemma-enriched preparations from canine ventricle. *Circ. Res.* 55:676–688.

Hamill, O. P., A. Marty, E. Neher, B. Sakmann, and F. J. Sigworth. 1981. Improved patch-clamp techniques for high-resolution recording from cells and cell-free membrane patches. *Pflügers Arch.* 391:85–100.

Harrison, S. M., and D. M. Bers. 1987. The effect of temperature and ionic strength on the apparent Ca-affinity of EGTA and the analogous Ca-chelators BAPTA and dibromo BAPTA. *Biochim. Biophys. Acta.* 925: 133–143.

Hess, P., J. B. Lansman, and R. W. Tsien. 1986. Calcium channel selectivity for divalent and monovalent cations. *J. Gen. Physiol.* 88:293–319.

Hove-Madsen, L., and D. M. Bers. 1992. Indo-1 binding to protein in permeabilized ventricular myocytes alters its spectral Ca binding properties. *Biophys. J.* 63:89–97.

Hove-Madsen, L., and D. M. Bers. 1993. Passive Ca buffering and SR Ca uptake in permeabilized rabbit ventricular myocytes. *Am. J. Physiol.* 264: C677–C686.

Jahnke, U., and L. M. G. Heilmeyer, Jr. 1980. Comparison of the Mg^{2+} and Ca^{2+} binding properties of troponin complexes P^1-TI_2C and TI_2C *Eur. J. Biochem.* 111:325–332.

Janczewski, A. M., and E. G. Lakatta. 1993. Buffering of calcium influx by sarcoplasmic reticulum during the action potential in guinea-pig ventricular myocytes. *J. Physiol.* 471:343–363.

Kirby, M. S., Y. Sagara, S. Gaa, G. Inesi, W. J. Lederer, and T. B. Rogers. 1992. Thapsigargin inhibits contraction and Ca^{2+} transient in cardiac cells by specific inhibition of the sarcoplasmic reticulum Ca^{2+} pump. *J. Biol. Chem.* 267:12545–12551.

Konishi, M., and J. R. Berlin. 1993. Ca transients in cardiac myocytes measured with a low affinity fluorescent indicator, furaptra. *Biophys. J.* 64:1331–1343.

Konishi, M., A. Olson, S. Hollingworth, and S. M. Baylor. 1988. Myoplasmic binding of fura-2 investigated by steady-state fluorescence and absorbance measurements. *Biophys. J.* 54:1089–1104.

LaBelle, E. F., and E. Racker. 1977. Cholesterol stimulation of penetration of unilamellar liposomes by hydrophobic compounds. *J. Membr. Biol.* 31:301–315.

Martell, A. E., and R. M. Smith. 1974. Critical Stability Constants. Vol. 1: Amino Acids. Plenum Publishing Corp., New York. 199–269.

Melzer, W., E. Rios, and M. F. Schneider. 1987. A general procedure for determining calcium release from the sarcoplasmic reticulum in skeletal muscle fibers. *Biophys. J.* 51:849–863.

Mitra, R., and M. Morad. 1985. A uniform enzymatic method for dissociation of myocytes from heart and stomachs of vertebrates. *Am. J. Physiol.* 249:H1056–H1060.

Miyata, H., H. S. Silverman, S. J. Sollott, E. G. Lakatta, M. D. Stern, and R. G. Hansford. 1991. Measurement of mitochondrial free Ca^{2+} concentration in living single rat cardiac myocytes. *Am. J. Physiol.* 261: H1123–H1134.

Moravec, C. S., and M. Bond. 1991. Calcium is released from the junctional sarcoplasmic reticulum during cardiac muscle contraction. *Am. J. Physiol.* 260:H989–H997.

Ogawa, Y. 1985. Calcium binding to troponin C and troponin: effects of Mg^{2+}, ionic strength and pH. *J. Biochem.* 97:1011–1023.

Page, E. 1978. Quantitative ultrastructural analysis in cardiac membrane physiology. *Am. J. Physiol.* 235:C147–C158.

Pan, B.-S., and R. J. Solaro. 1987. Calcium-binding properties of troponin C in detergent-skinned heart muscle fibers. *J. Biol. Chem.* 262: 7839–7849.

Pierce, G. N., K. D. Philipson, and G. A Langer. 1985. Passive calcium-buffering capacity of a rabbit ventricular homogenate preparation. *Am. J. Physiol.* 249:C248–C255.

Post, J. A., G. A. Langer, J. A. F. Op Den Kamp, and A. J. Verkleij. 1988. Phospholipid asymmetry in cardiac sarcolemma. Analysis of intact cell and "gas-dissected" membranes. *Biochim. Biophys. Acta.* 943:256–266.

Robertson, S. P., J. D. Johnson, and J. D. Potter. 1981. The time-course of Ca^{2+} exchange with calmodulin, troponin, parvalbumin, and myosin in response to transient changes in Ca^{2+}. *Biophys. J.* 34:559–569.

Sagara, Y., and G. Inesi. 1991. Inhibition of the sarcoplasmic reticulum Ca^{2+} transport ATPase by thapsigargin at subnanomolar concentrations. *J. Biol. Chem.* 266:13503–13506.

Solaro, R. J., R. M. Wise, J. S. Shiner, and F. N. Briggs. 1974. Calcium requirements for cardiac myofibrillar activation. *Circ. Res.* 34:525–530.

Sommer, J. R., and R. A. Waugh. 1976. The ultrastructure of the mammalian cardiac muscle cell—with special emphasis on the tubular membrane systems. *Am. J. Pathol.* 82:192–221.

Wendt-Gallitelli, M. F., and G. Isenberg. 1991. Total and free myoplasmic calcium during a contraction cycle: x-ray microanalysis in guinea-pig ventricular myocytes. *J. Physiol.* 435:349–372.

Wier, W. G., T. M. Egan, J. R. López-López, and C. W. Balke. 1994. Local control of excitation-contraction coupling in rat heart cells. *J. Physiol.* 474:463–471.

Zhou, Z., and E. Neher. 1993. Mobile and immobile calcium buffers in bovine chromaffin cells. *J. Physiol.* 469:245–273.

Zot, H. G., and J. D. Potter. 1987. Calcium binding and fluorescence measurements of dansylaziridine-labeled troponin C in reconstituted thin filaments. *J. Muscle Res. Cell Motil.* 8:428–436.